Electron Densities in Jupiter's Outer Magnetosphere Determined from Voyager 1 and 2 Plasma Wave Spectra

B.L. Barnhart[1], W.S. Kurth[1], J.B. Groene[1], J.B. Faden[1], O. Santolik[2], and D.A. Gurnett[1]
[1]Department of Physics & Astronomy, The University of Iowa, Iowa City, IA, USA
[2]Faculty of Mathematics and Physics, Charles University, Prague, Czech Republic

Abstract

This paper presents a data set of electron plasma densities in Jupiter's outer magnetosphere derived from high-resolution wideband measurements of low-frequency radio and plasma waves obtained by Voyagers 1 and 2 during their 1979 flybys. This work utilizes a new data processing tool that makes important improvements in the identification of the plasma frequency and other characteristic frequencies of the plasma, thereby allowing for the determination of the electron density within the Jovian magnetosphere.

Using the theory of cold plasmas and criteria based upon previous studies, we establish an extensive set of reasoning for interpreting cutoffs and resonances in the spectra of non-thermal continuum radiation, Z-mode emissions, and whistler mode emissions to identify characteristic frequencies of the plasma including the electron plasma frequency, R=0 cutoff, L=0 cutoff, upper hybrid resonance frequency, and the electron cyclotron frequency. While most regions in Voyager plasma wave data are cases where $f_{pe}>f_{ce}$, this investigation analyzes time periods where $f_{pe}<<f_{ce}$ to interpret the various cutoffs and resonances in the spectrum. The resulting data set for the electron densities, in regions where $f_{pe}>f_{ce}$ and $f_{pe}<<f_{ce}$, has higher temporal resolution than any others that exist today.

Introduction

Nonthermal continuum radiation is prevalent in the outer regions of both the terrestrial and Jovian magnetospheres. Data from the Imp 6 and Imp 8 missions were used to demonstrate that this electromagnetic radiation propagates in the ordinary mode above a lower cutoff frequency at the local electron plasma frequency [Gurnett and Shaw, 1973; Gurnett, 1975]. Similar electromagnetic radiation was first discovered at Jupiter using the Voyager Plasma Wave Receiver [Scarf et al., 1979; Gurnett et al., 1979]. These emissions have been used to infer the plasma density in the Jovian magnetosphere [Scarf et al., 1979; Gurnett et al., 1979; Barbosa et al., 1979; Gurnett et al., 1980]. However, the only attempt to systematically determine the plasma density using high resolution wideband waveform data was by Ansher et al., [1992].

The nonthermal continuum radiation found at Jupiter spans frequencies higher and lower than the solar wind plasma frequency. Emissions at frequencies greater than the solar wind frequency propagate freely out of the magnetosphere while the lower frequencies are trapped between the higher frequency boundaries of the magnetopause and the dense inner regions of the magnetosphere [Gurnett et al., 1980; Gurnett et al., 1981].

The trapped continuum radiation exhibits a lower cutoff, below which no waves propagate [Gurnett and Shaw, 1973; Stix, 1992] and this cutoff is interpreted as an upper limit for the electron plasma frequency (f_{pe}), which is proportional to the local electron plasma density by the relation

$$f_{pe} = 8980\sqrt{n_e} \quad (1)$$

where f_{pe} is in Hz and the electron density n_e is in cm^{-3} [Stix, 1992]. The plasma frequency is just one of several characteristic frequencies defined in cold plasma theory. Others are the electron cyclotron frequency f_{ce}, the right and left hand cutoffs $f_{R=0}$ and $f_{L=0}$, and the upper hybrid resonance frequency f_{UH}. These frequencies are related to one another by the following formulas:

$$f_{ce} = 28|B| \quad (2)$$

$$f_{R=0} = \frac{f_{ce}}{2} + \sqrt{(f_{pe})^2 + \left(\frac{f_{ce}}{2}\right)^2} \quad (3)$$

$$f_{L=0} = -\frac{f_{ce}}{2} + \sqrt{(f_{pe})^2 + \left(\frac{f_{ce}}{2}\right)^2} \quad (4)$$

$$f_{UH}^2 = f_{pe}^2 + f_{ce}^2 \quad (5)$$

In (2) |B| is the magnitude of the magnetic field in nT and the units of all frequencies are in Hz.

Figure 1 is a sketch of the characteristic frequencies of the plasma as a function of distance from Jupiter. The distance axis is not to scale, but is designed to show the situation in the plasma sheet where the electron plasma frequency f_{pe} is greater than f_{ce} and another region, representative of the lobe of the magnetosphere, where f_{ce} is greater than f_{pe}.

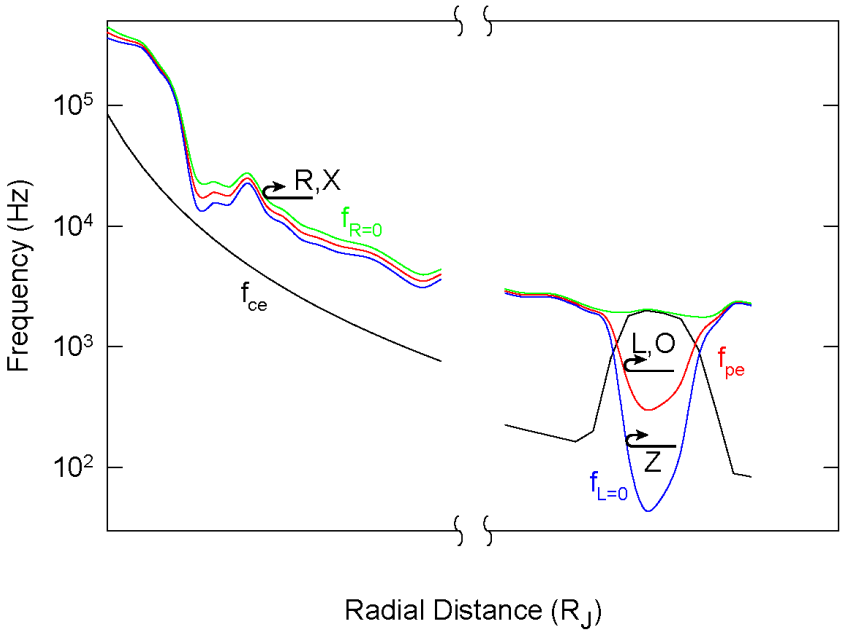

Figure 1: Sketch of the characteristic frequencies found in the Jovian magnetosphere. Displays two separate regions where $f_{pe} > f_{ce}$ and where $f_{pe} << f_{ce}$ and illustrates the relationships between the various cutoffs.

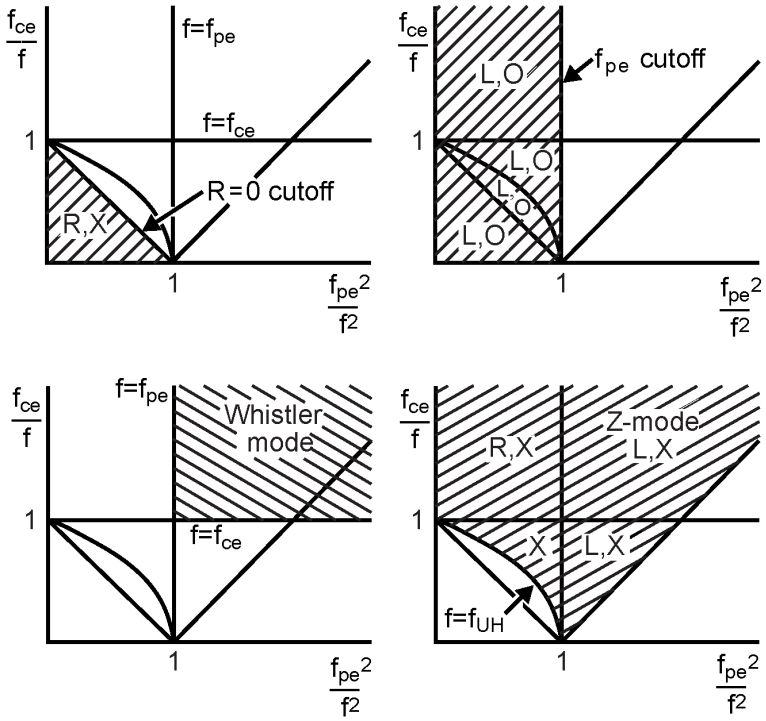

Figure 2: Frequency plots after Gurnett and Bhattacharjee [2005] illustrating the theoretically allowed propagation of various wave modes. Also, the characteristic frequencies of these modes (representing cutoffs or resonances) are displayed. The frequencies are defined in (1) – (5) and f is the frequency of the plasma.

Figure 2, after Gurnett and Bhattacharjee [2005], illustrates four distinct wave modes which are designated by the waves' polarization and electric field component's orientation with respect to the local magnetic field. Conventionally, the polarization is labeled as either L for left-handed polarization or R for right-handed polarization. Also, the orientation of the electric field component is labeled either O for ordinary, meaning parallel to the local magnetic field or X for extraordinary, meaning perpendicular to the local magnetic field. Thus, we have four modes possible: the left-handed ordinary mode (L,O), the left-handed extraordinary mode (L,X) otherwise known as the Z-mode, the right-handed extraordinary mode (R,X), and the whistler mode.

Each mode propagates within a certain frequency range, as displayed in Figure 2, and exhibits a cutoff where its index of refraction goes to zero, and some can experience resonances such as the upper hybrid resonance, as in (5).

The cyclotron frequency can be accurately determined from magnetometer measurements making f_{ce} known almost everywhere wideband data exists. In the simplest spectra, only the non-thermal continuum radiation needs to be considered and we interpret the low-frequency cutoff of this emission as the electron plasma frequency as previously assumed by Shaw and Gurnett [1980], Moses et. al. [1987], and Barbosa et. al. [1990]. In fact, this cutoff is strictly an upper limit to the local electron plasma frequency due to the potential of a high density region existing between the radio emission source and the spacecraft. When this occurs, the cutoff measurement pertains to the distant density structure rather than the local cutoff. However, the cutoffs measured are usually sharp which suggests a local cutoff [Gurnett et. al., 1981]. In a more complex spectrum consisting of a mix of both ordinary and extraordinary modes, the continuum radiation may exhibit a partial cutoff at somewhat higher frequencies than the plasma frequency, which can be interpreted as the cutoff of the extraordinary mode at $f_{R=0}$. In other cases, Z-mode radiation is observed at lower frequencies [Kennel et. al. 1987; Barbosa et. al., 1990]; the low-frequency cutoff of this emission is at $f_{L=0.}$ Occasionally, an enhancement is seen near the low-frequency cutoff of the continuum radiation and corresponds to the upper hybrid resonance frequency f_{UH}. Given the relations above, it is clear that if one characteristic frequency can be identified, one can determine f_{pe} and an estimate of the electron density can be made.

We will discuss a new electron density data set generated using a new, semi-automated analysis tool. The data set represents the highest resolution measurements of the electron density at Jupiter. We will also comment on the accuracy and limitations of the density measurements. We will discuss the methods and criteria used in selecting the various characteristic frequencies. In many instances, two or more of the characteristic frequencies can be identified at a given time. This provides an opportunity to check for consistency between the multiple identifications to both validate the interpretation of the characteristic frequencies, and to assess the accuracy of the density determination.

For a full description of the Voyager 1 and 2 plasma wave instrumentation, see Scarf and Gurnett [1977].

New Analysis Tools

Previous attempts to derive electron densities from the Voyager wideband data were carried out one spectrum at a time with a high level of human intervention. This was tedious and time intensive and subject to inconsistent identifications of the cutoffs. For the development of this data set, we developed tools to automatically identify cutoffs and resonances with only minimal guidance from the operator. The increase in efficiency

allowed the temporal resolution to be set not by how time intensive the work was, but by how long spectra needed to be averaged to produce a relatively clean spectrum. For this work, we chose to average the spectrum over 1 second increments. Figure 3 shows diagnostic displays associated with two new analysis tools used to find cutoffs and peaks within spectra. The tools and the processes by which they work are described below.

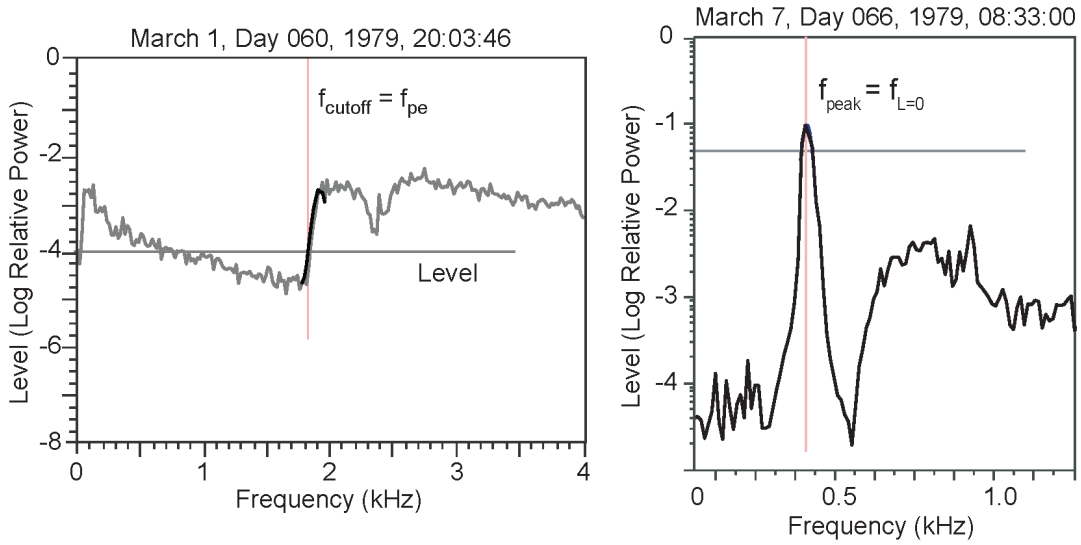

Figure 2: Examples displaying results from the new cutoff and peak detection tools. Left panel shows f_{pe} measured from the sharp cutoff of the power spectrum at approximately 1.8 kHz. Right panel shows the detection of a peak in the spectrum interpreted as $f_{L=0}$.

Cutoff Detector

Previously, Ansher et. al. [1992] produced a preliminary electron density data set by identifying the plasma frequency and therefore the electron density in the Jovian magnetosphere. This data set provided information on sharply defined density structures found in the plasma sheet. Ansher et al. [1992] used wideband waveform observations taken from Voyager 1 and 2 that provide high resolution spectra of the nonthermal continuum radiation. The identification process used by Ansher et al. [1992] was a manually-intensive, subjective technique requiring the operator to manually identify the plasma frequency cutoff from 4-s averaged spectra. Ansher et al. [1992] mention the extraordinary time involved with producing such a data set by hand.

Further development of this density determination process has yielded significant success and improvement from the previous method. The present investigation utilizes a new program that allows the operator to highlight the general vicinity of the cutoff on a frequency-time spectrogram. Then, an algorithm finds the cutoff in the region and records the frequency at 1 second intervals. Hence, the automated procedure allows an increase in temporal resolution of a factor of four and significantly reduces both manual effort and subjective judgment by the operator.

The cutoff detection algorithm is controlled by a small number of parameters that can be set by the operator. The first parameter is the cutoff level. In determining possible cutoff candidates, the algorithm scans the region highlighted by the operator and records two separate points, one above the cutoff level and one below. The closer the two points are temporally, the steeper the slope will be. Therefore, the operator can change the

location of the cutoff level to manipulate where the algorithm looks for cutoffs within the highlighted region of interest.

The next parameter is the slope magnitude, which designates the minimum magnitude of the finite difference slope where the cutoff must reside. The operator may raise the slope level in order to scan only for sharp cutoffs, or lower it in order to accommodate less steep slopes, depending on the quality of the spectrum data.

The cutoff level, slope magnitude and cutoff candidates are displayed by the program for viewing by the operator. When there is more than one possible cutoff, the detection program will display the possible cutoffs. While the algorithm chooses the lowest frequency cutoff by default, the operator may override the algorithm and choose any of the possible cutoffs.

Since the Fourier transform parameters used to produce the spectra yield a spectral resolution of 28 Hz, this represents the ultimate accuracy with which the cutoff can be determined. Below we discuss consistency checks when two or more characteristic frequencies can be determined and used to determine f_{pe} independently. The different values can be compared and typically agree to several 10's of Hz. Almost all cases agree to within 100 Hz. The uncertainty in f_{pe} translates into a variable uncertainty in the plasma density and is greater in a relative sense when the plasma frequency is low. For example, if we assume an error of 100 Hz in any measurement, a measurement at 300 Hz produces a 70% fractional uncertainty in the density. However, if the measurement is made at 3 kHz, then the fractional uncertainty of the density is much smaller, approximately 7%.

In order to record the confidence of the cutoff frequency measurements, data quality indices were given to each data. The indices range from 0 to 3 with 0 being a cutoff with the highest confidence and 3 being the least. The amount of noise in the spectrum dictates the quality rating given to a particular data point. Points with a minimal amount of noise are given values of 0, whereas points where the spectral noise is so great that the cutoff is unclear are given a 1 or 2 index depending on the severity of the noise.

A data quality index of 3 is given when there are obstructions in the spectrum blocking the ability for an accurate measurement, or where there is such a significant amount of background spectral noise that the spectra must be time-averaged over a longer period of time in order to interpret the cutoff. For example, the Voyager wideband receivers have notch filters that are used to suppress interference at the power supply frequency of 2.4 kHz and its third harmonic. When a cutoff resides near a notch filter, a data quality index of 3 is used. While the notch filters do not span more than 200 Hz, any measurement made near them is uncertain.

The data set described below allows users to select the confidence level of the data they would like to use. That is, for very accurate measurements an operator can select only low data quality indices when using the data, and for a more complete data set where absolute accuracy is less important, one can choose to include those with poorer quality indices.

The Peak Detector

The program also uses an algorithm for peak detection. Many spectra of interest to this study include Z-mode radiation, which has a low-frequency cutoff at $f_{L=0.}$ As pointed out by Barbosa et al. [1990], the Z-mode is often narrowbanded and peaks at this frequency. As the intensity of this peak increases, the width of the emission appears to broaden because of limitations in the Fourier transform and the low dynamic range of the

4-bit waveform system on Voyager. Barbosa et al. [1990] demonstrated that taking the peak of the Z-mode as $f_{L=0}$ yields the highest consistency in the determination of f_{pe}. Hence, when the Z-mode is enhanced, we utilize the peak detection algorithm to identify $f_{L=0}$ from which f_{pe} and the electron density can be derived using (4). This algorithm can also be used to determine f_{UH} when an enhancement at that frequency is present in the spectrum.

The peak detection algorithm fits a Gaussian curve to the highest peak within the region specified by the program operator. The program then records the frequency of the Gaussian's peak. In order to determine an estimate of the measurement's error, the full-width at half maximum of the Gaussian curve is measured and recorded along with its peak frequency. The narrower the peak is, the more accurate the measurement will be. This quantitative method is superior to the quality data indices described above. However, to provide a consistent data set we have also translated the width of the peak to quality indices by assigning an index of 0 for $0 < \Delta f \leq 20$ Hz, 1 for $20 < \Delta f \leq 35$ Hz, 2 for $35 < \Delta f \leq 50$ Hz, and 3 for $\Delta f > 50$ Hz.

While the operator utilizes a color spectrogram to guide the cutoff and peak detectors, we emphasize that this is only used as a means of identifying the appropriate range in frequency for the algorithm to search. The direct use of color spectrograms tends to mislead an operator to perceive a cutoff that is not equivalent to the cutoff in the actual power spectrum [Barbosa et al., 1990]. Because this may lead to a systematic error in the data, the algorithm utilizes the spectrum itself, and does not depend on a color scale to determine the characteristic frequencies. This should reduce systematic error and lead to more accurate results.

Data Coverage

This data set does not provide complete coverage of the time intervals when the Voyager spacecraft were within Jupiter's magnetosphere. Two criteria must be met before a determination of the electron density can be made. First, wideband waveform data must exist. These data provide high spectral and temporal resolution measurements of the wave spectrum below 12 kHz but require large telemetry rates in order to return the measurements to the ground. In fact, these data compete with Voyager imaging data for the downlink resource. Hence, the data are only available a fraction of the time. When available, they exist in 48-second 'frames' which may be continuous, periodic, such as one 48-second frame out of every four such frames, or simply present sporadically. Second, spectral features which exhibit a cutoff or resonance related to the electron density must be present. By far the most prevalent emission of use is the non-thermal continuum radiation. It literally fills the magnetosphere between the magnetopause and higher density regions of the inner magnetosphere. Typically, continuum radiation is not present inside of approximately 20 to 25 Jovian radii R_J. Figure 4 shows the coverage of the density data compiled in this investigation for both Voyager 1 and 2 as projected into the ecliptic plane.

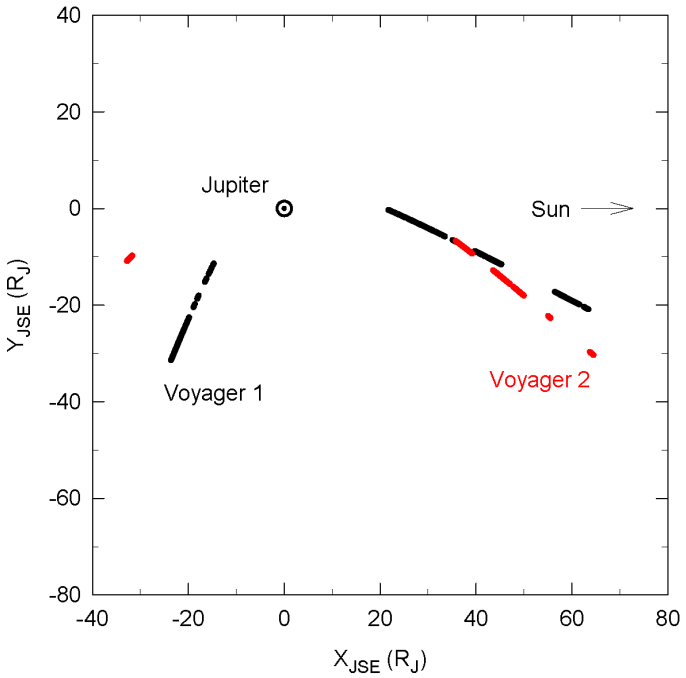

Figure 4: Plot displaying density data coverage for Voyager 1 and 2. Each point represents one minute where density data was determined using this plasma wave investigation.

While the present investigation focuses on the outer magnetosphere, the works of Scarf et al. [1979] and Birmingham, et al. [1981] have shown that in the inner magnetosphere, other wave phenomena such as the upper hybrid resonance band can be used to infer the plasma density. For future investigations, this same peak detection tool can be used to accurately determine the plasma density.

The next section discusses in detail the identification of the above-mentioned cutoffs and resonances and a consistent set of interpretations of complex spectra, often including Z-mode and whistler emissions in addition to the continuum radiation.

Continuum Radiation with One Cutoff

The simplest spectra to interpret for the purposes of determining the electron density are those that include non-thermal continuum radiation with a clear low frequency cutoff and with no other emissions near this such as the example displayed in Figure 5. For the purposes of this data set, we agree with the Gurnett et al. [1981] interpretation that based upon PWS data it is appropriate to assume that the continuum radiation cutoff is f_{pe} and using (1) we can accurately determine the local electron plasma density. Throughout this paper, the plasma frequency identified in this way will be operationally defined as the observed f_{pe} as opposed to the calculated f_{pe}, which is derived using (2) through (5). When there is only one cutoff present in the continuum radiation, we have assumed that the continuum radiation is propagating in the ordinary mode and that the cutoff is indeed the plasma frequency. An alternate possibility would be to identify this cutoff as the R=0 cutoff at $f_{R=0}$. But, most theories [Shaw and Gurnett, 1980; Moses et. al., 1987; Barbosa et al., 1990] favor the L,O mode as the continuum radiation, hence, we assume that there is always at least some L,O component present when the continuum radiation is detected.

Figure 5 shows Voyager 1 data from 1979 day 060, beginning at 20:05. The plasma frequency is shown as a white trace at the low-frequency cutoff of the continuum radiation. The cutoff detection algorithm has been used to determine f_{pe} and the plasma density is calculated using (1).
Figure 6 is a plot of the electron density for the same time interval as Figure 5, using the determination of f_{pe} and (1). Below, we discuss spectra which exhibit continuum radiation with two different cutoffs.

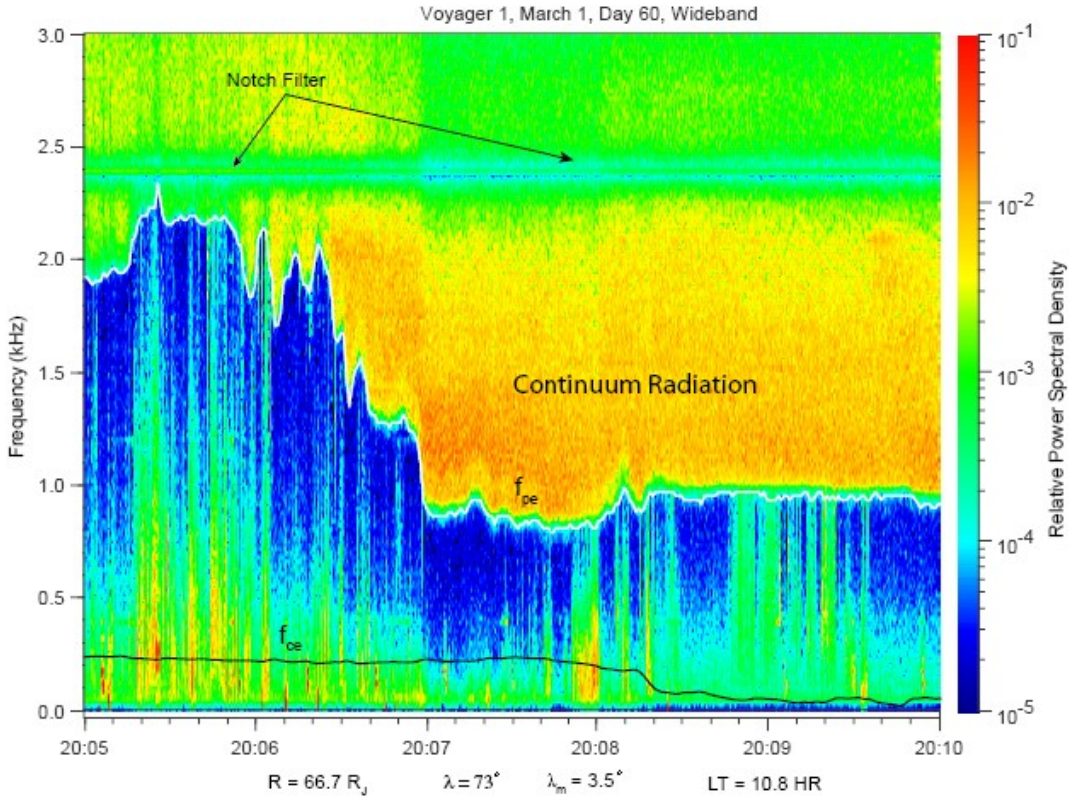

Figure 5: Continuum radiation propagating through the Jovian magnetosphere with a cutoff at f_{pe}. Notice that this is a region where $f_{pe} > f_{ce}$. The notch filter, occurring at 2.4 kHz disrupts cutoff measurements for a brief time near 20:05:25.

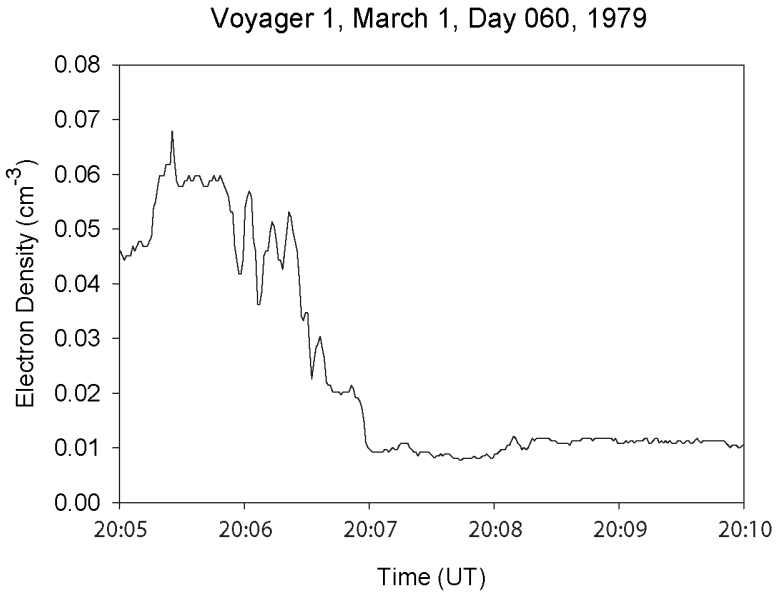

Figure 6: Electron densities determined from the Voyager 1 time period displayed in Figure 5. The density is determined by measuring f_{pe} with the cutoff analysis tool and using (1),.

Continuum Radiation with Two Cutoffs

While our data set includes accurate measurements of the observed f_{pe}, and therefore the local electron plasma density, we also found other cutoffs that occur in the data that could be helpful in determining the local electron density. One such situation occurs when two cutoffs are apparent in the continuum radiation spectrum, as is the case in Figure 7. On day 063, at 11:54:30, we have identified the low-frequency cutoff as f_{pe} and observe a second cutoff, at somewhat higher frequencies.

The low frequency cutoff is at 4.27 kHz and the higher cutoff is at 4.87 kHz, which is 600 Hz higher. For this time period f_{ce} is about 1.1 kHz. If we take f_{pe} to be the low frequency cutoff, and use (2) and (3) to calculate $f_{R=0}$, it is apparent that the calculated value of $f_{R=0}$ is approximately 4.8 kHz, very close to the observed upper frequency cutoff. This confirms that the lower frequency cutoff is indeed f_{pe} and the upper frequency cutoff is $f_{R=0}$, the cutoff of the R,X mode. This process is reciprocal, meaning that the use of the algorithm to identify the R,X cutoff and calculating f_{pe} is equivalent to and equally valid as using the cutoff at the plasma frequency, directly.

The spectrum can become even more complicated when Z-mode radiation is present. Next, we will discuss these circumstances.

Weak Broadband Z-mode Radiation

At 11:54:52 on Day 063, shown in Figure 7, a weak low frequency emission is present along with the continuum radiation with cutoff at f_{pe} and at $f_{R=0}$ as discussed above. This is characteristic for many of the time periods recorded throughout the Jovian plasma sheet. We first assume that the low frequency cutoff of the broadband Z-mode radiation is $f_{L=0}$ as discussed in Barbosa et al. [1990]. Taking $f_{L=0}$ equal to 3.69 kHz and f_{ce} equal to 1.1 kHz, and using (4), we calculate a value for f_{pe} to be 4.20 kHz, which is very close to the previously observed f_{pe}. This result agrees with the Barbosa [1990] interpretation of the cutoff of this broadband radiation to be the L=0 cutoff frequency.

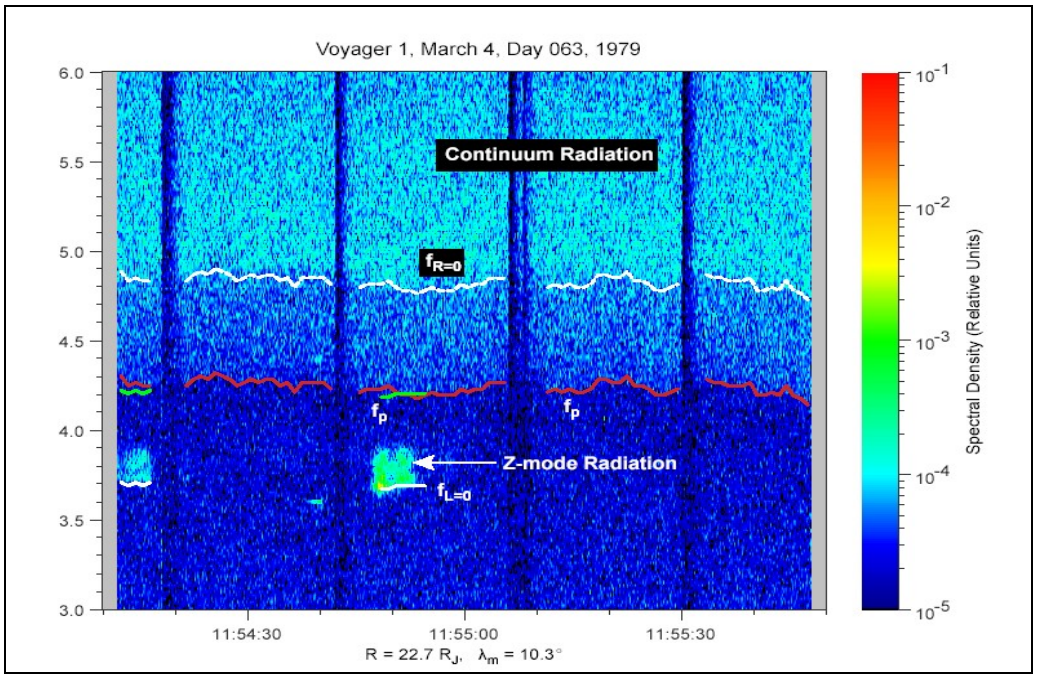

Figure 7: Spectrogram displaying continuum radiation with two cutoffs where $f_{R=0}$ is calculated from the observed f_{pe}. Also, a correct interpretation for f_{pe} calculated from an observed Z-mode radiation cutoff at $f_{L=0}$ is demonstrated.

Conversely, if f_{pe} is assumed and $f_{L=0}$ is calculated using (4) the values similar to the measured $f_{L=0}$ are found.

Figure 7 demonstrates that f_{pe} calculated from the cutoff of the broadband Z-mode radiation is consistent with the observed plasma frequency. Thus, it can be inferred that in regions where the plasma frequency is not apparent, it is possible to use (2) and (4) to calculate the theoretical value for the plasma frequency from the cutoff of low intensity broadband Z-mode emissions and use (1) to determine the local electron density.

Intense Narrowband Z-mode Radiation

Another common occurrence found in both the Voyager 1 and 2 data is an intensification of the narrowband Z-mode radiation. Barbosa et al., [1990] argued that taking the peak of the narrowband Z-mode radiation as $f_{L=0}$ gave the most consistent results. For this investigation we have found our data to be consistent with the interpretation given by Barbosa et al., [1990] that where the Z-mode is intense and narrowbanded, as opposed to the weak, broadband emission in Figure 7, we assume $f_{L=0}$ is the frequency at the peak of the Z-mode.

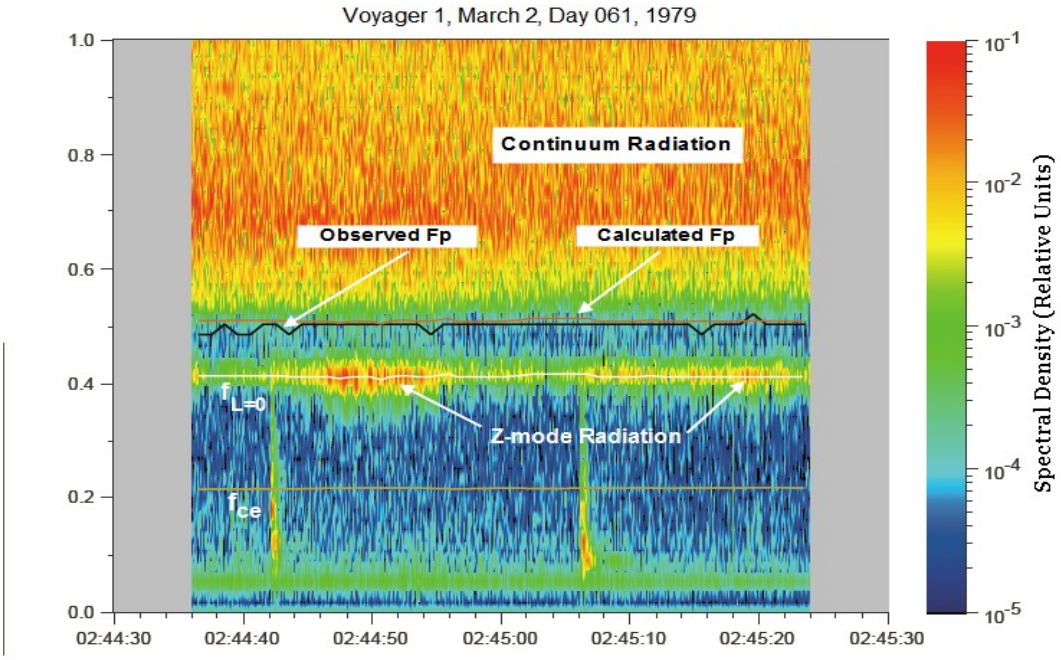

Figure 8: Intense, narrowband Z-mode radiation. Interpreting the peak of the Z-mode band as the L=0 frequency yields a calculated f_{pe} that is consistent with the observed f_{pe}.

To demonstrate our agreement with Barbosa et al. [1990], we look to another example shown in Figure 8. The time period during Voyager 1, day 061 from 2:44:30 to 2:45:30 shows intense narrowband Z-mode radiation where f_{pe} is also apparent. Figure 8 shows a white line identifying the peak of the narrow band Z-mode radiation which we have interpreted as $f_{L=0}$. The electron cyclotron frequency is displayed for reference. Notice that the calculated plasma frequency, which was obtained from the observed $f_{L=0}$ using (4), is consistent with the observed f_{pe} to within ~20 Hz. Using this interpretation for the L,O mode and calculating the plasma frequency gives results consistent with the cutoff at f_{pe}. Note that, again, this process is entirely reciprocal, meaning either $f_{L=0}$ or f_{pe} can act as the observed frequency and be used with (2) and (4) to derive the other frequency.

During some time periods, there is an overlap of continuum radiation and Z-mode emissions, obscuring f_{pe} and making it difficult to determine f_{pe} directly. Hence, the use of $f_{L=0}$ extends our ability to accurately determine the local electron density for time periods where the continuum radiation and Z-mode emissions are blended such that the cutoff at f_{pe} is obscured.

Situations when $f_{pe} << f_{ce}$

As Voyager approaches the lobe of the magnetosphere, the density as well as f_{pe} drops precipitously and approaches or even drops below f_{ce}. Perraut et al. [1998] studied a similar case obtained by the Galileo plasma wave instrument. Using the Galileo sweep frequency receiver data, they located a region where $f_{pe} << f_{ce}$ and provided an identification of the various characteristic frequencies exhibited in the spectrum.

Within the Voyager 1 data set, the most prominent region where $f_{pe} << f_{ce}$ occurs during day 065 between 7:00 and 12:00. This is during an outbound pass from a distance

of 18.5 R_J to 22.5 R_J. Similar to the example shown by Perraut et al. [1998], the spectrum of these regions exhibit three distinct emissions in the frequency range of 28 Hz to a few kilohertz.

Because the wideband data downlink resource is shared with the Voyager imaging instrument, there are large data gaps within this time period. However, between day 065 07:45 and 10:00 as well as between 11:00 and 11:25, there are high resolution wideband data where $f_{pe} << f_{ce}$. Figure 9 displays this entire time period with f_{ce} shown as the black line. Notice that as the density drops, f_{ce} climbs to approximately 2 kHz, which is much greater than f_{pe}. We will look more closely at three specific regions (labeled 1, 2, and 3 in Figure 9) and determine the characteristic frequencies in each region.

The first region, labeled Region 1 in Figure 9 with a detailed view in Figure 10, exhibits three distinct intense low frequency bands at less than 1.5 kHz. Figure 10 displays a few minutes of day 065 data starting at 08:07:30. The cutoffs are located, from lowest frequency to highest, at approximately 86 Hz, 360 Hz, and 960 Hz. Interpreting the middle frequency as $f_{L=0}$ (white line) and calculating f_{pe} (red line), results in cutoffs that are consistent with the observed cutoffs at 360 and 960 Hz. The wideband receiver has a high-pass filter at 50 Hz; hence, it is likely the cutoff at 86 Hz is related to this filter. Thus, we conclude that continuum radiation propagates down to approximately 960 Hz and cuts off at f_{pe}. Below this exists Z-mode radiation which cuts off at approximately 360 Hz and whistler mode emissions which extend below $f_{L=0}$. This enables us to accurately determine the density for this region.

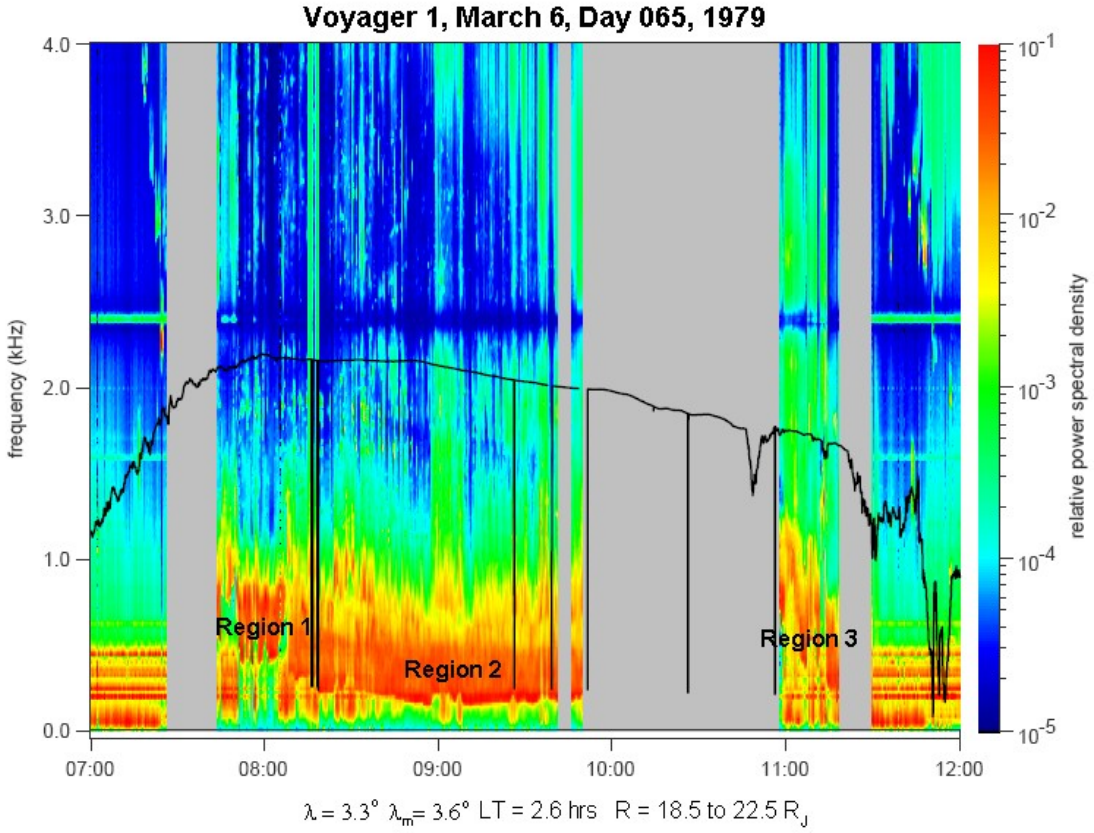

Figure 9: Extended period when $f_{pe} << f_{ce}$. The black line denotes the cyclotron frequency. For each region, there is a consistent interpretation for the characteristic frequencies, including f_{pe}. Thus, we can determine the plasma frequency in each of these regions.

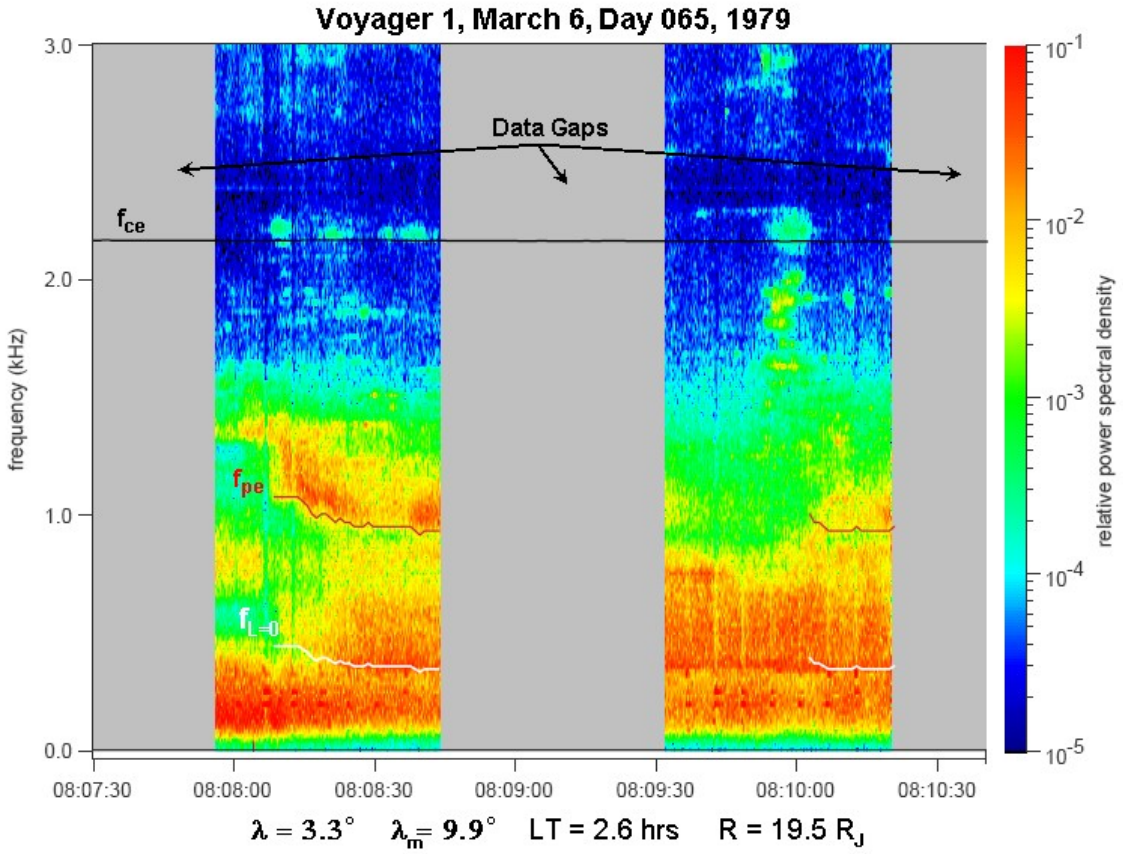

Figure 10: Interpretations of characteristic frequencies by assuming the middle cutoff at 360 Hz to be $f_{L=0}$. Using (2) and (4), we calculate f_{pe} and find that it matches the frequency of the higher frequency cutoff quite well. When we assume the middle cutoff is f_{pe}, we find that neither the calculated $f_{R=0}$ nor $f_{L=0}$ match the cutoffs near 86 or 960 Hz.

Region 2 in Figure 9 with a detailed view in Figure 11 is another example where $f_{ce} >> f_{pe}$ and where there are three intense low frequency bands with distinct cutoffs. We utilize a similar approach as used with Region 1 and postulate that the cutoff of the highest frequency band, at approximately 900 Hz, is f_{pe}. Looking at Figure 11, on day 065 at 09:35:58, it is clear that the calculated value for $f_{L=0}$ (from the measured f_{pe}, (2) and (4)) is consistent with the middle cutoff frequency at approximately 350 Hz. We conclude that again continuum radiation propagates down to a low frequency cutoff at f_{pe}, near 900 Hz, Z-mode radiation propagates further down to $f_{L=0}$ at approximately 350 Hz, and below this exist whistler mode emissions. The lowest cutoff is likely an instrumental effect caused by the high pass filter at 50 Hz.

Another example which is similar occurs at 09:38, however, a gap in magnetometer data makes the determination of f_{ce} problematic, hence, no calculated frequencies can be determined. However, since the power spectrum is similar to the former case and f_{ce} is not varying prior to the gap, we conclude that the plasma properties are similar to those of three minutes prior. Therefore, the same interpretation should apply.

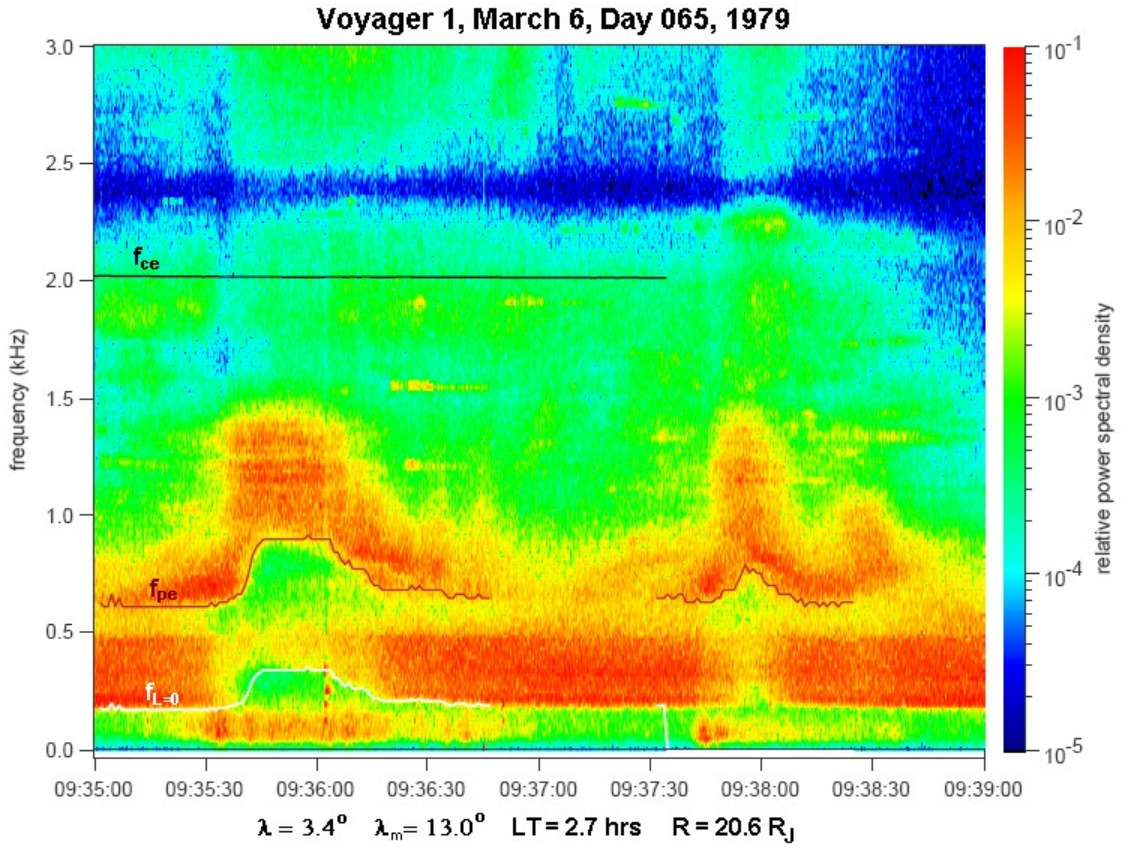

Figure 11: A consistent hypothesis for the interpretation of these three frequency bands in a region 20.6 R_J where the $f_{pe} << f_{ce}$. The upper band is continuum radiation with a lower cutoff at f_{pe}, the middle band is the Z-mode with a lower cutoff at $f_{L=0}$, and the lower band must be the whistler mode.

Region 3, shown in Figure 12, exhibits a serendipitously placed upper hybrid resonance emission occurring at 1.8 kHz from 11:08 to 11:09 and also between 11:11 and 11:12 where f_{ce} is approximately 1.7 kHz, just below the UHR bands. We use the peak of f_{UH} and (2), (3), and (5) to calculate both f_{pe} and $f_{L=0}$. At 11:08, if we assume f_{UH} to be 1.8 kHz, the calculated f_{pe} corresponds to the cutoff of the intense emission at approximately 500 Hz. Thus, we conclude that the lower frequency emission is a mixture of both Z and whistler modes. A similar example can be found from 11:11 to 11:12. Here, the identification of the cutoff near 300 Hz consistently identifies the lower frequency band as the Z-mode with $f_{L=0}$ near its peak.

Using the fortunate occurrence of spectra as in Figures 10-12 we were able to unambiguously determine the electron plasma density in Regions 1, 2, and 3. We then assumed continuity of the spectral features to time periods in Figure 9 where there is only one cutoff apparent. Thus, we were able to determine the density for a majority of the time in Figure 9. We used a similar technique for other regions where $f_{pe} << f_{ce}$. Moses et al. [1987] and Perraut et al. [1998] previously studied low resolution Voyager data and Galileo plasma data, respectively, where the $f_{pe} << f_{ce}$ and which contained three low frequency bands similar to the high resolution Voyager data in this study. Their interpretations for these emissions and characteristic frequencies are consistent with our observations.

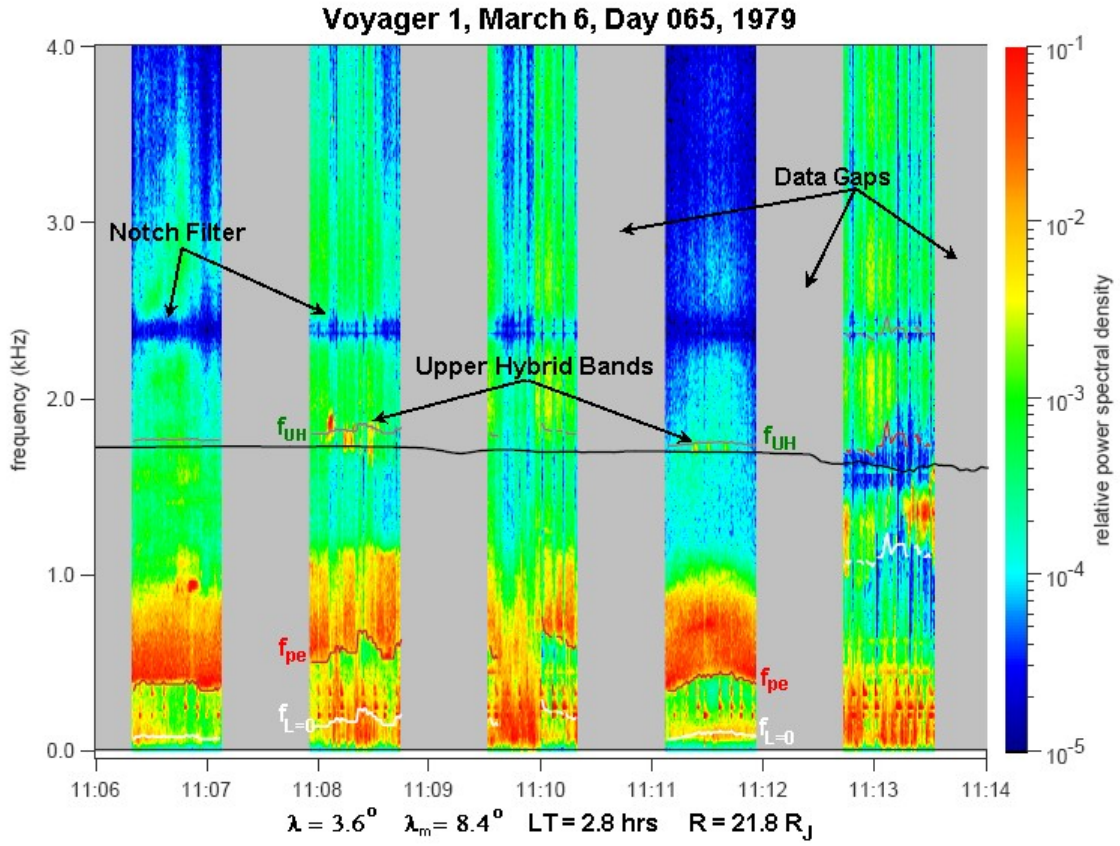

Figure 12: Upper hybrid resonance bands are present along with two unidentified lower frequency bands. Using f_{ce}, (2), (4) and (5), we calculate f_{pe} and $f_{L=0}$. The calculated frequencies match features in the power spectrum, giving a consistent interpretation for f_{UH}, f_{pe} and $f_{L=0}$ when the $f_{pe} << f_{ce}$.

Summary and Discussion

The purpose of this investigation is to provide an accurate, high resolution plasma density data set for regions in the Jovian magnetosphere based upon Voyager 1 and 2 plasma wave data [Gurnett et al., 1979]. Throughout the investigation, it was necessary to employ certain interpretations of the data in order to accurately measure and determine the characteristic frequencies (f_{UH}, f_{pe}, $f_{L=0}$, $f_{R=0}$, f_{ce}). Using the electron plasma frequency, we were able to accurately compute the local electron density for a substantial amount of time given by the Voyager 1 and 2 plasma wave data. In regions where a clean cutoff at f_{pe} was not apparent, it was necessary to invoke interpretations for other spectral features, including the extraordinary mode, and Z modes to calculate the local electron density. In regions where both f_{pe} and either the extraordinary or Z modes were present, two characteristic frequencies could be used along with the equations of cold plasma theory to validate the mode identifications.

We found that our data was most consistent when we interpreted the cutoff of the nonthermal continuum radiation to be the plasma frequency as described by Gurnett et al. [1973]. Also, when there is a low intensity broadband emission present, interpreting the low frequency cutoff as $f_{L=0}$ gives a consistent estimate of f_{pe}. However, when there is an intense narrowband Z-mode emission present, interpreting the peak frequency as $f_{L=0}$ gives a consistent estimate of f_{pe}. When two or more characteristic frequencies were present, we checked for consistency between them. In most cases, the agreement was

well within 100 Hz. If there were inconsistencies greater than 100 Hz, we deemed our assumptions incorrect. The consistency checks, when possible, led us to conclude that we had made the correct interpretations of the more complex spectra. However, in cases where there existed a mix of continuum radiation, Z-mode emissions, and the whistler mode, we verified our interpretation at times when these consistency checks were possible and then interpreted nearby spectra with only one clear cutoff in a self-consistent manner. We must warn that there is no irrefutable method to verify all of our interpretations. The final data set will be submitted to the Planetary Data System (PDS) in May 2007 and made available to the scientific community.

The Data Set

The data set consists of ASCII files with one record per time step. Each record includes the time, the electron cyclotron frequency (if available), the frequency of the cutoff or resonance, a code indicating which cutoff or resonance was determined, the calculated electron density, and a set of position coordinates for the spacecraft at the time of the observation. Also included in each record are f_{pe}, $f_{R=0}$, $f_{L=0}$, f_{UH}, and the quality index. One of these four frequencies is just a copy of the observed cutoff or resonance frequency. Different files are used for each day.

Acknowledgments

This research was supported by NASA through Grant #NNG05GG98G.

References

Barbosa, D.D., W.S. Kurth, S.L. Moses, and F.L. Scarf, Z mode radiation in Jupiter's magnetosphere: the source of Jovian continuum radiation, *J. Geophys. Res.,* 95, 8187-8196, 1990.

Gurnett, D.A., The earth as a radio source: The nonthermal continuum, *J. Geophys. Res.*, 80, 2751, 1975.

Gurnett, D.A. and A. Bhattacharjee, *Introduction to Plasma Physics: With Space and Laboratory Applications*, Cambridge University Press, Cambridge, 2005.

Gurnett, D.A., F.L. Scarf, W.S. Kurth, R.R. Shaw, and R.L. Poynter, Determination of Jupiter's electron density profile from plasma wave observations, *J. Geophys. Res.*, 86, 8199-8212, 1981.

Gurnett, D.A., and R. R Shaw, Electromagnetic radiation trapped in the magnetosphere above the plasma frequency, *J. Geophys. Res.,* 78, 8136-8149, 1973.

Gurnett, D.A., W.S. Kurth, and F.L. Scarf, Plasma wave observations near Jupiter: Initial results from Voyager 2, *Science, 206,* 987, 1979.

Gurnett, D.A., W.S. Kurth, and F.L. Scarf, The structure of the Jovian magnetotail from plasma wave observations, *Geophys. Res. Letters*, 7, 53-56, 1980.

Kennel, C.F., R.F. Chen, S.L. Moses, W.S. Kurth, F.V. Coroniti, F.L. Scarf, and F.F. Chen, Z mode radiation in Jupiter's magnetosphere, *J. Geophys. Res.,* 92, 9978, 1987.

Scarf, F.L., and D.A. Gurnett, A plasma wave investigation for the Voyager mission, *Space Sci. Rev.,* 21, 289, 1977.

Scarf, F.L, D.A. Gurnett, and W.S. Kurth, Jupiter plasma wave observations: An initial Voyager 1 overview, *Science, 204,* 991, 1979.

Shaw, R.R., and D.A. Gurnett, A test of two theories for the low-frequency cutoffs of nonthermal continuum radiation, *J. Geophys. Res.,* 85, 4571-4576, 1980.

Stix, T.H., *The Theory of Plasma Waves*, McGraw-Hill, New York, 1962.

Moses, S.L., W.S. Kurth, C.F. Kennel, F.V. Coroniti, and F.L. Scarf, Polarization of Low-Frequency Electromagnetic Radiation in the Lobes of Jupiter's Magnetotail, *J. Geophys. Res.*, 92, 4701-4705, 1987.

Perraut, S., A. Roux, P. Louarn, D.A. Gurnett, W.S. Kurth, and K.K. Khurana, Mode conversion at the Jovian plasma sheet boundary, *J. Geophys. Res.*, 103, 14995-15000, 1998.